Spectrochimica Acta Part A: Molecular and Biomolecular Spectroscopy 184 (2017) 7–12

Contents lists available at ScienceDirect

Spectrochimica Acta Part A: Molecular and Biomolecular Spectroscopy

journal homepage: www.elsevier.com/locate/saa

A turn-on type stimuli-responsive fluorescent dye with specific solvent effect: Implication for a new prototype of paper using water as the ink

Xiaochen Hu [a], Yang Liu [b], Yuai Duan [a], Jingqi Han [a], Zhongfeng Li [a], Tianyu Han [a,*]

[a] *Department of Chemistry, Capital Normal University, 100048 Beijing, P.R. China*
[b] *Beijing Key Laboratory of Radiation Advanced Materials, Beijing Research Center for Radiation Application, 100015 Beijing, P.R. China*

ARTICLE INFO

Article history:
Received 19 January 2017
Received in revised form 26 April 2017
Accepted 27 April 2017
Available online 29 April 2017

Keywords:
Water-based ink
Water-sensitive
Fluorescent dye
Solvent effect
Paper

ABSTRACT

In this study, we reported the photoluminescence (PL) behaviour of a new intramolecular charge transfer (ICT) compound, ((E)-2-(((2-hydroxynaphthalen-1-yl)methylene)amino)benzoic acid, (HABA), which shows ICT solvent effect in aprotic solvents as confirmed by absorption and emission spectra. While in protic solvents including water and ethanol, the charge transfer (CT) band significantly reduces. Remarkable fluorescence enhancement in the blue region was also observed for HABA in polar protic solvents. We described such phenomena as "specific solvent effect". It can be ascribed to the hydrogen bonding formation between HABA and protic solvents, which not only causes significant reduction in the rate of internal conversion but also elevates the energy gap. Density functional theory (DFT) calculations as well as the dynamics analysis were performed to further verify the existence of hydrogen bonding complexes. Stronger emission turn-on effect was observed on HABA solid film when it is treated with water and base solution. The stimuli-responsive fluorescence of HABA enables a new green printing technique that uses water/base as the ink, affording fluorescent handwritings highly distinct from the background. Thermoanalysis of the dye suggests the nice thermostability, which is highly desired for real-world printing in a wide temperature range.

© 2017 Published by Elsevier B.V.

1. Introduction

Although we are currently in an age inundated with electronic information, paper and ink still play an important role in our daily life. According to a study, the printing ink market is growing by 3% per year, leading to an increasing demand for traditional as well as new printing inks [1]. Inks are generally composed of four ingredients, including colorant, binder, solvent and additives. The colorant, mostly aromatic compound with hyperchrome units, is obviously the key component. Unfortunately, it is easy to be photobleached, resulting in color fading in long-term storage [2]. Additionally, the toxicity of the colorant poses a health risk and causes environmental pollution with daily use [3–4]. Nanoparticles fabricated by noble metals represent an efficient way to bestow yellow to red coloration, making themselves good candidates for new inks [5–8]. They enjoy much higher light fastness compared with organic dyes or pigments. However, a strong limitation to such type of inks stem from their high cost, even if efficient coloring performance can be achieved with very low concentrations. So it is difficult for them to be commercialized.

It is an exceptionally elegant way to imprint chromophores on the solid substrate (paper, polymer matrix and quartz plate, etc.) to fabricate the "paper", where printing or handwriting can be performed by using specific stimulants (commonly nontoxic) as the "ink" [9–12]. In this manner, store, collection and recycle of the involved hazardous materials, if any, will become easier, as they are in solid state. The stimuli-responsive property is the first necessity of such chromophores. Research efforts have been made to identify new stimuli-responsive chromophores that can be used in the manufacture of printing in order to reduce dependency on traditional dyes and lessen the environmental impact. Among such materials, the ones responding to mechanical force [13–14], voltage [15], light [16], ions [17] and acid/alkali [18–19], have been intensely studied, as they are more green and easy to access.

In our previous work, we have reported an archetype of ink-free rewritable paper based on a mechanochromic luminogen [20]. Letters or complex patterns can be written repeatedly on such paper. Unfortunately, it often requires extremely high pressure to planish the molecular conformation of the mechanochromic luminogens in order to change their emission/absorption. A quantitative study reported by Tian et al. states that a full color change can only be realized under a pressure as high as 78,164 times greater than the standard atmospheric pressure [21]. On the other hand, most of the stimuli-responsive materials containing mechanochromic luminogens, however, function in a "turn-off" mode: an initially emissive dye becomes non-emissive when it gets stimulated. Correspondingly, "turn-on" type materials are more

---

[*] Corresponding author.
E-mail address: phanw@163.com (T. Han).

http://dx.doi.org/10.1016/j.saa.2017.04.079
1386-1425/© 2017 Published by Elsevier B.V.

welcome as they are more sensitive and less likely to generate false-positive signals [22–24]. Herein we report a turn-on type fluorescent dye with water-sensitive nature. We studied the PL behaviour, the specific solvent effect and the related mechanism. The main goal of this study is to design an archetype of paper that uses water as the ink.

2. Experimental Section

2.1. Materials and Methods

Chemicals involved were purchased from Aldrich and used as received without further purification. Ethanol was distilled from magnesium under nitrogen prior to use. High resolution mass spectra (HRMS) were recorded on a GCT premier CAB048 mass spectrometer operated in MALDI-TOF mode. ^{1}H NMR and ^{13}C NMR spectra were measured on a Varian VNMRS 600 MHz spectrometer (internal reference: tetramethylsilane). UV–vis spectra were recorded on a SHIMADZU UV 2550 spectrophotometer. PL spectra were recorded on a HITACHI F-7000 FL spectrophotometer. The ground-state geometries were optimized using DFT with MPWB1K/aug-cc-pVTZ//MPWB1K/6–31 + g* and B3LYP/6–31 + g*. Conductor-like polarizable continuum model (CPCM) was employed to estimate the solvent-solute interaction. All the calculations were performed using the Gaussian 05 package. Thermogravimetric analysis (TGA) was carried on a TGA Q5000 under air at a heating rate of 10 °C/min. Thermal transitions of the luminogen were investigated by differential scanning calorimetry (DSC) using a TA DSC Q1000 under air at a heating rate of 10 °C/min.

2.2. Synthesis

As shown in Scheme 1, to a round-bottom flask containing 2-hydroxy-1-naphthaldehyde (2 g, 11.60 mmol, 1 equiv) was added anhydrous ethanol (200 ml), 2-aminobenzoic acid (1.60 g, 11.60 mmol, 1 equiv). Two drops of acetic acid (Scheme 1) was added to the reaction mixture before it was heated to 60 °C. After stirring for 8 h, the resulting precipitate was collected by vacuum filtration using ethanol and hexane to rinse, yielding HABA ((E)-2-(((2-hydroxynaphthalen-1-yl) methylene)amino)benzoic acid) as a yellow-orange solid powder (yield: 61%). Structural analysis including ^{1}H NMR, ^{13}C NMR and ESI-Mass spectra are listed in the supporting information (Fig. S1-S3), the corresponding data are represented as follows:

^{1}H NMR (600 MHz, DMSO-d$_6$) δ: 13.40 (br s, 1H), 9.34 (s, 1H), 8.36–8.35 (d, 1H), 7.97–7.94 (q, 2H), 7.83–7.81 (d, 1H), 7.69–7.67 (t, 2H), 7.48–7.45 (t, 1H), 7.34–7.26 (m, 2H), 6.78–6.77 (t, 1H) (abbreviation: br = broad, s = singlet, d = doublet, t = triplet, q = quartet, m = multiplet).

^{13}C NMR (600 MHz, DMSO-d_6) δ: 176.32, 167.81, 151.51, 143.30, 138.89, 134.30, 134.10, 131.59, 129.47, 128.69, 126.84, 125.63, 124.79, 123.99, 122.17, 120.65, 119.47, 109.21.

HRMS (MALDI-TOF): m/z 292.0974 $[(M + H)^+$, calcd 292.0974].

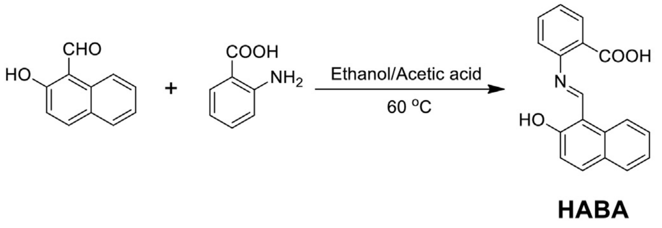

Scheme 1. Synthetic route to HABA.

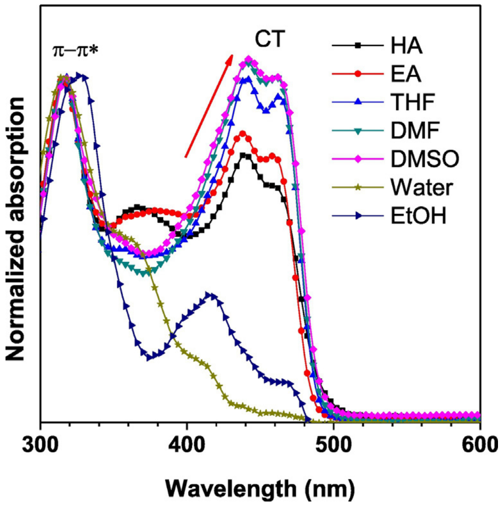

Fig. 1. UV–vis absorption spectra of HABA in different organic solvents. Concentration: 10 μM. Abbreviation: hexane (HA), ethyl acetate (EA), tetrahydrofuran (THF), N, N-dimethylformamide (DMF), dimethyl sulfoxide (DMSO), ethanol (EtOH).

3. Results and Discussion

3.1. Solvent Effect

HMAB possesses electron donor (D, phenolic hydroxyl) and acceptor (A, benzoic acid) groups, as well as the single bonds (C—C and C—N) capable of triggering geometry transition that can affect the energy level. The introduction of D-A pairs will thus endue a fluorogen with distinct solvatochromic effects. In most cases, a polar solvent brings the luminogen from the locally excited (LE) state to the CT state and then stabilizes the resulting CT state by solvation. Consequently, the energy gap between the ground and excited state will be narrowed, giving rise to red-shifted emission/absorption spectra. The good solubility of HABA allows us to investigate its photophysical properties in the solvents with varying polarities. The absorption peak of HABA appears at around 316 nm in hexane, corresponding to the π-π* transition (Fig. 1). The shoulder peak at 439 nm can be ascribed to CT transition. Similar to the absorption spectrum in hexane, HABA shows the dual-absorption band in other solvents, too. The hypochromic peaks represent the LE state absorption, closely related to the π-π* transition, while the bathochromic peaks denote the CT band. The former remains

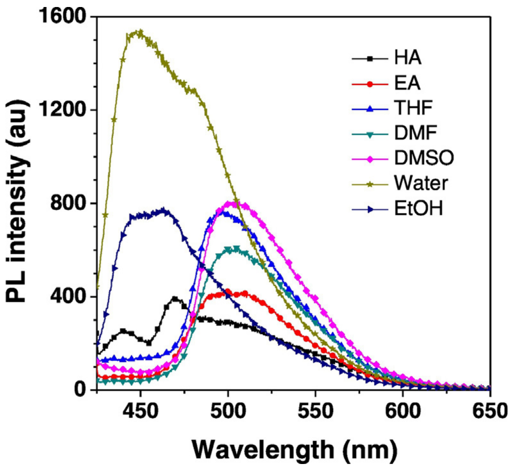

Fig. 2. PL spectra of HABA in different organic solvents. Concentration: 5 mM. Excitation wavelength: 410 nm.

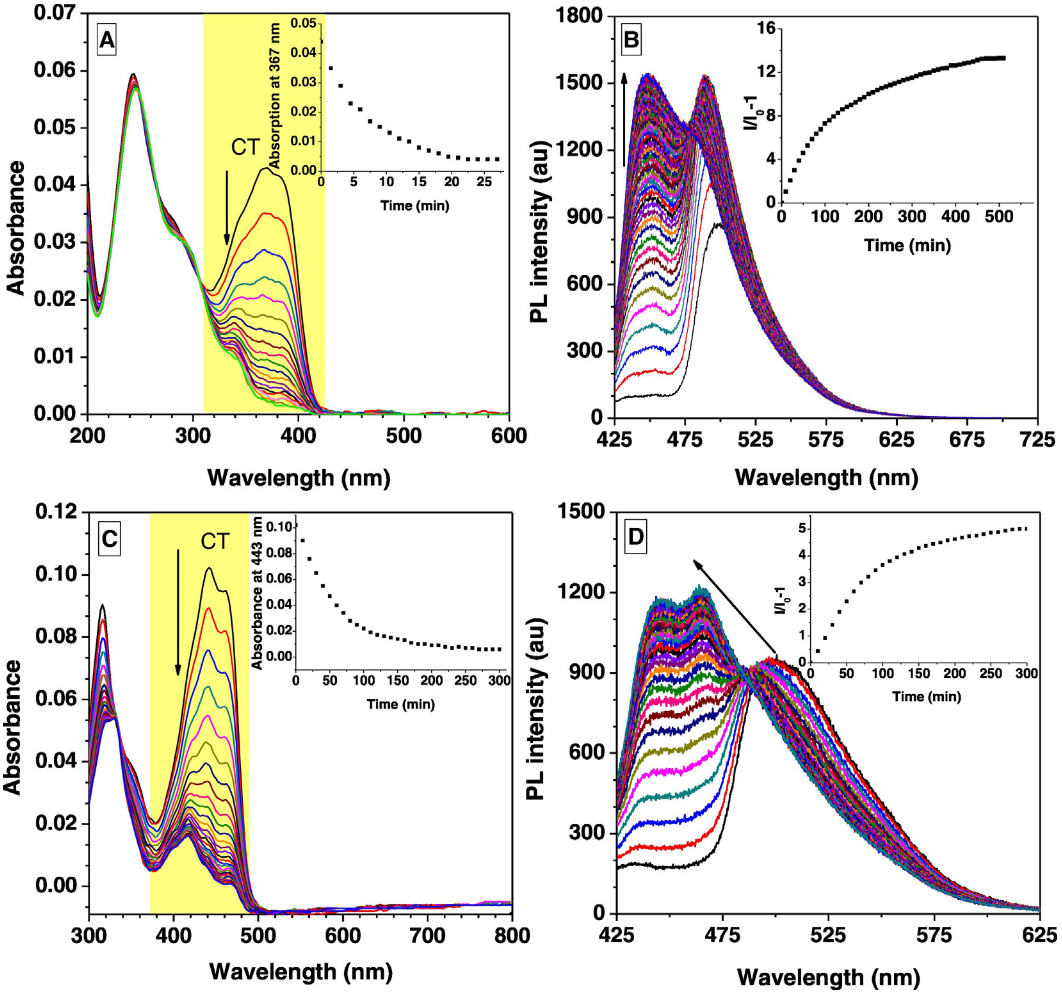

Fig. 3. Time-dependent absorption spectra of HABA in aqueous solution (A) and EtOH (C) (10 μM); Time-dependent PL spectra of HABA in aqueous solution (B) and EtOH (D) (5 mM). Excitation wavelength: 410 nm. Insets for A–D: corresponding tendency plots.

nearly unchanged in various solvents, however, the latter is remarkably enhanced as the solvent polarity gradually increases, and turns into the dominant absorption band in polar solvents such as DMF and DMSO.

In protic solvents including water and ethanol, the CT band becomes inconspicuous. Such type of solvent effect was occasionally observed with chromophores containing hydrogen bonding sites such as aniline

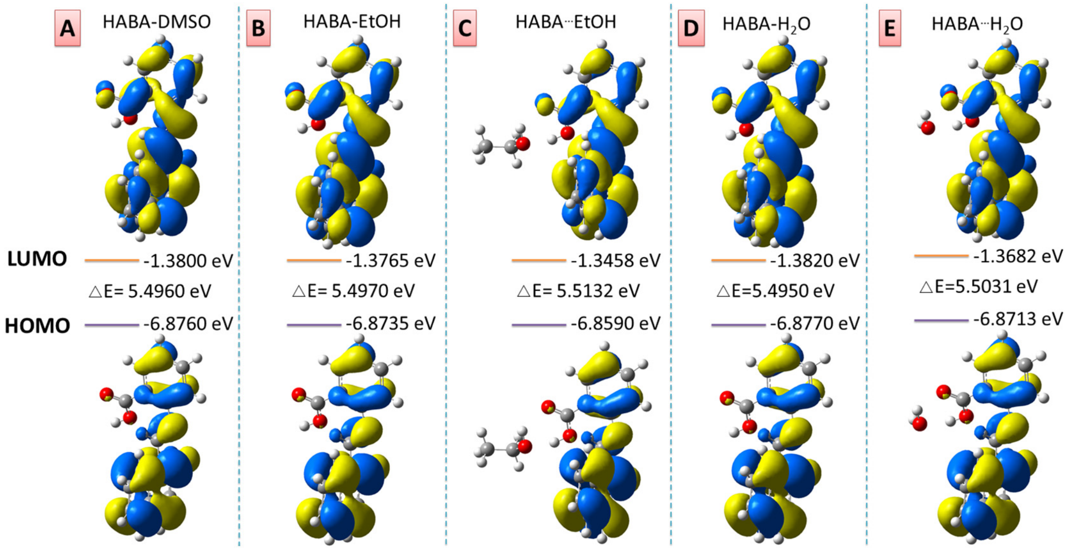

Fig. 4. Molecular orbital amplitude plots of HOMO and LUMO energy levels of (A) HABA-DMSO (HABA in CPCM model with DMSO) (B) HABA-EtOH (HABA in CPCM with EtOH), (C) HABA···EtOH (HABA forming hydrogen bonding in EtOH in CPCM model), (D) HABA-H_2O (HABA in CPCM model with water), (E) HABA···H_2O (HABA forming hydrogen bonding in water in CPCM model), calculated at the MPWB1K/aug-cc-pVTZ//MPWB1K/6–31 + g* level.

and carboxylic acid derivatives [25–27]. It has been reported that hydrogen bonding between solute-solvent often affects the photodynamic properties of chromophores as well as their static spectral properties [28]. There are at least three hydrogen bonding sites: carboxylic acid, phenolic hydroxyl and imine), the latter two are less likely to bond with solvents as enol-imine unit is normally a six-membered, hydrogen-bonded pseudo ring [12,29–30]. As a hydrogen bond donor, the hydroxyl group of water and ethanol is readily to form hydrogen bonding with carbonyl acid, as the latter, not only a lone pair electrons owner but also a hydrogen donor, will serve as a strong hydrogen bonding site. The electronegativity on carbonyl group is thus reduced upon bonding with hydrogen, resulting in a relatively weaker electronic withdrawing ability. In this manner, D-A efficacy is suppressed, giving rise to a larger energy gap intrinsic to the LE state. Based on the above discussion, the reduction of CT band in water and ethanol probably rises from hydrogen bonding complexes.

The fluorescence spectra of HABA were also measured in solvents with different polarities and hydrogen bond donating abilities to determine the solvent effect (Fig. 2). Evidently, the light emission is red-shifted in wavelength and enhanced in intensity with increasing solvent polarity when comparing the spectrum of HABA in HA, THF, DMF and DMSO. The red-shift is due to narrowed energy gap of CT transition when the molecule is surrounded by polar solvent [31]. The weakened fluorescence can be attributed to internal conversion, which is a non-radiative process caused by vibronic interactions between close-lying S1 and S2 states according to related studies [32–33]. As expected, remarkable fluorescence enhancement in the blue region was observed for HABA in polar protic solvents, as hydrogen bonding causes significant reduction in the rate of internal conversion [33].

3.2. Dynamic Analysis

The real-time change in absorption spectrum of HABA is shown in Fig. 3A. HABA was dissolved in water and the absorption was monitored over time. An absorption peak at 370 nm is observed with a freshly prepared aqueous solution, demonstrating the CT transition triggered by the solvent polarity. The CT absorption band gradually decreases with time, and remains almost unchanged after 20 min. The emission spectrum in water shows time-dependent nature as well: CT emission progressively blue-shifts and LE emission at 448 nm arises (Fig. 3B). Isotherm of the emission intensity at 448 nm plotted in the inset of Fig. 3B shows that the growth trend levels off after 460 min. The dynamics analysis of HABA indicates the formation of hydrogen bonding complex. In the first stage, there's not enough time to form hydrogen bond between HABA and water, hence CT transition plays a major role. When HABA molecules turn into hydrogen bonding complexes, LE state will predominate. The EtOH solution of HABA shows the similar spectral response: drop of CT absorption band, increased LE state emission and blue-shifted wavelength in both absorption and emission spectra (Fig. 3C–D). In addition, the absorption spectrum of HABA in EtOH changes visibly slower than that observed with aqueous solution, as the hydrophilicity of benzoic acid moiety makes it easier to bond with water compared with EtOH. The time-dependent absorption and emission spectra in DMSO shown in Fig. S4, by contrast, exert no obvious change, indicating the absence of solute-solvent hydrogen bond in this aprotic solvent where CT solvation effect plays the dominant role.

3.3. DFT Calculations

It has been reported that the MPWB1K method is fully fit for analyzing weak interactions, especially hydrogen bonding [34–35]. So we performed such method in order to seek out more evidences to explain the specific solvent effect in protic solvent. Highest occupied molecular orbital (HOMO) and (lowest unoccupied molecular orbital) LUMO are plotted and displayed in Fig. 4. HOMO orbital of HABA in DMSO-CPCM model mainly locates on aromatic rings, while the carboxylic acid group, where the conjugation are much weakened relative to the former, are excluded from electron delocalization (Fig. 4A). The LUMO orbital partly shifts to carboxylic acid owning to its electronic withdrawing ability. Calculations in EtOH-CPCM model (without regard to intermolecular hydrogen bonding) give a similar electronic cloud distribution and energy gap (Fig. 4B). Apparently the results disagree with the spectral behaviour shown in Figs. 1 and 2. But if the hydrogen bonding between HABA and EtOH was taken into consideration in EtOH-CPCM model, the energy gap will rises from 5.4970 to 5.5132 eV (Fig. 4C), which matches well with the hypochromatic shift in both absorption and emission spectra (Figs. 1 and 2). As the most polar solvent, water is supposed to activate the CT transition as well, leading to an asymmetric electronic cloud distribution. As shown in Fig. 4D, the HOMO and LUMO orbitals together with the energy gap (5.4950 eV) calculated by using CPCM model likewise (without hydrogen bonding), are very close to that in DMSO (Fig. 4A). It is quite clear that this single-molecule model is inappropriate, as disproved by the spectral responses to water (Figs. 1 and 2). Therefore we calculated the HABA···H_2O hydrogen bonding complexes and found its energy gap (5.5031 eV) slightly increases as shown in Fig. 4E, corresponding to the blue-shift of HABA

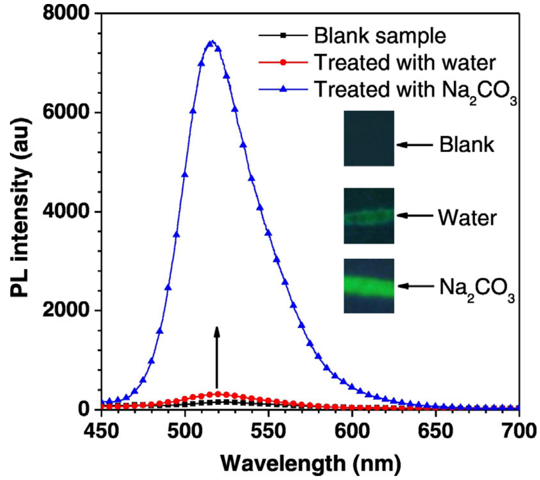

Fig. 5. Emission spectra of the pristine and water/alkali-treated HABA solid film. Excitation wavelength: 410 nm. Photographs were taken under UV illumination.

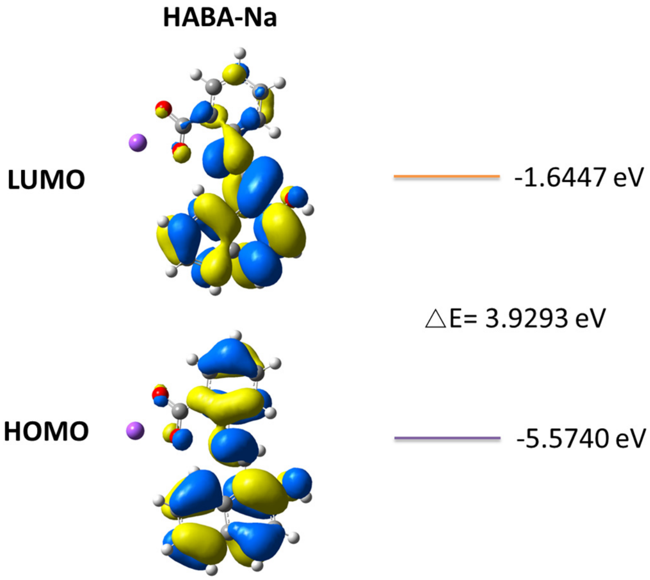

Fig. 6. Molecular orbital amplitude plots of HOMO and LUMO energy levels of the sodium carboxylate form of HABA (HABA-Na) calculated using B3LYP/6-31G* basis set.

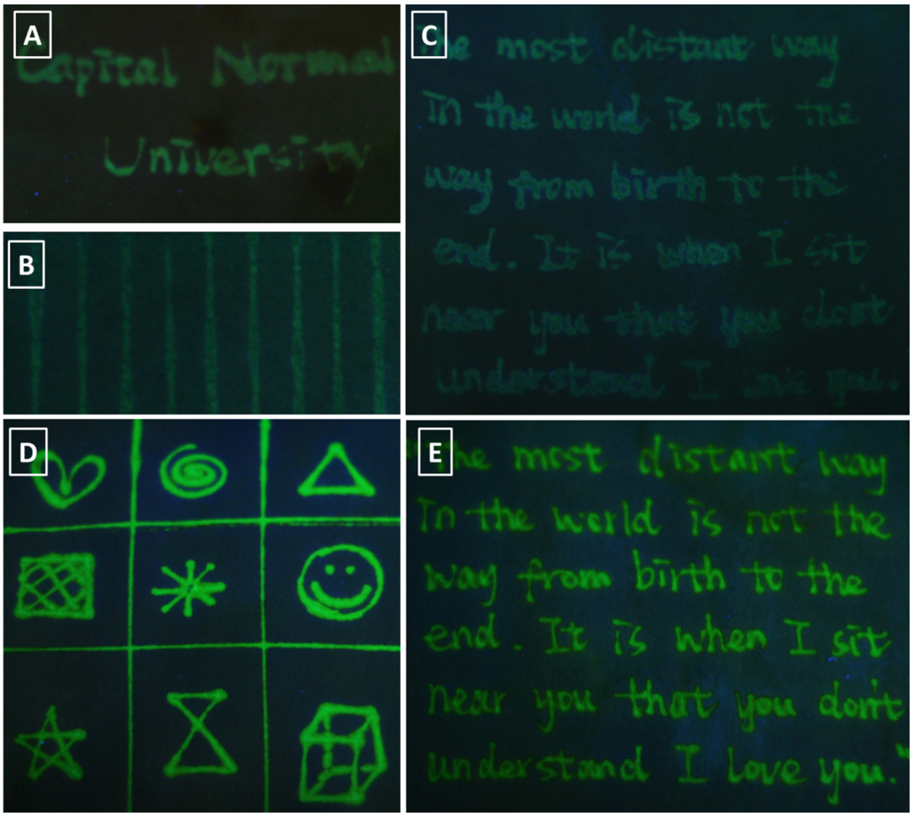

Fig. 7. Representative images taken under UV illumination showing fluorescent handwritings on the dye-loaded papers using water (A–C) and Na_2CO_3 (D–E) as the ink.

in water medium. The counter-examples shown in Fig. 4B and D, actually prove the existence of solvent-solute hydrogen bonding.

3.4. Stimuli-Responsive Fluorescence at Solid State

Inspired by the specific solvent effect with HABA, we try to achieve the water-sensitive property of this luminogen at solid state. A filter paper was immersed into a THF solution of HABA (5 mM) before dried in a vacuum oven, by which the dye was adsorbed onto a solid platform for PL measurements. The as-prepared sample exhibits a weak emission peaking at 523 nm (Fig. 5). The emission quenching can be ascribe to the plenary aromatic ring that favors π-π stacking and the following excimers, which is readily to consume the energy of excited molecule via nonradiative pathway. After the sample was dipped into water and dried, the fluorescence enhanced with a slight blue-shift (523–518 nm). On one hand, hydrogen bond formation suppresses nonradiative pathway including CT and internal conversion. On the other hand, molecular conformation and arrangement should be taken into consideration when discussing the emission at aggregation state. Inserting water molecules into HABA may enhance the steric hindrance, preventing the molecules from π-π stacking. Besides, the hydrogen bonding further restricts the intramolecular rotation to block the non-radiative pathway. In either case, the fluorescence will be boosted. However, the spectral response is less conspicuous than that in solution state as the solid-state reaction suffers from insufficient conversion due to weak physical contact between reagents [13].

After being dipped into an aqueous solution of Na_2CO_3 (0.1 M) and dried, the dye-loaded paper exhibits as high as 47-fold greater emission intensity enhancement relative to the starting sample (Fig. 5). The great signal enhancement can be easily observed by naked eyes as shown in

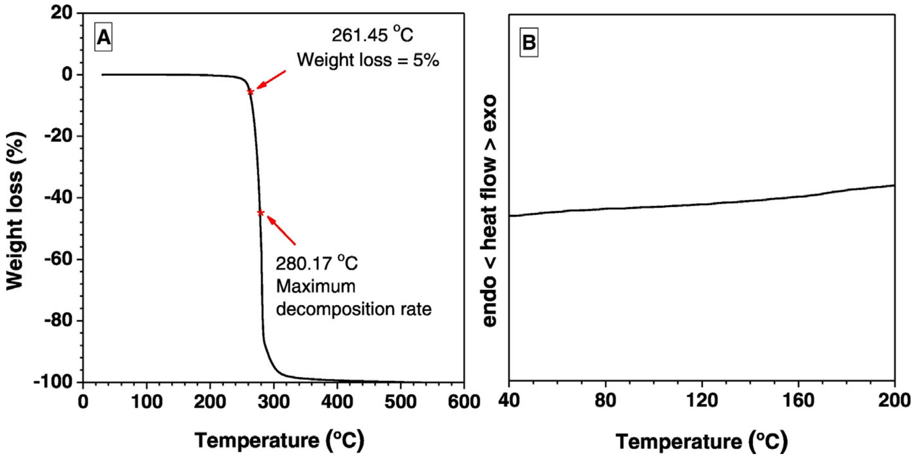

Fig. 8. TGA (A) and DSC (B) thermogram of HABA recorded under nitrogen at a heating rate of 10 °C/min.

the inset of Fig. 5. A hypochromatic shift (523–516 nm) was recoded as well. The spectral changes could be fit with that of water-treated sample because they share similar mechanisms. It is worth noting that the carboxylic acid group incorporated into the luminogen is apt to react with Na_2CO_3 to yield a deprotonated form, in which the molecules would be well dispersed owing to intermolecular electrostatic repulsion, offering the possibility of both conformational change and destruction of face-to-face packing. Therefore, the stronger emission induction observed with Na_2CO_3-treated sample is due to higher reactivity of the HABA with base solution than that with water.

HOMO and LUMO orbitals of the carboxylate form (HABA-Na) were plotted in Fig. 6. The energy levels of both HOMO and LUMO (especially HOMO) are dramatically elevated on account of the additional electron that will raise the interelectronic kinetic energy. HOMO electrons are delocalized on the entire molecule while in the LUMO orbital, electrons cease to migrate to the carboxylic moiety as the uncharged molecules do, because it is no longer an electron withdrawing group due to electrostatic repulsion. Destruction of D-A effect gives rise to a higher energy gap (3.9293 eV), avoiding the pathway including CT and internal conversion. The above DFT calculations agree well with the fluorescence changes, further providing theoretical support for the stimuli-responsive nature.

3.5. Text and Patterns Using Water/Base as the Ink

The stimuli-responsive fluorescence of HABA enables a new printing technique that uses water/base as the ink. Representative photos of a data writing process are listed in Fig. 7. Blank paper was prepared simply by dipping a filter paper into a THF solution of HABA (5 mM). The text or patterns were written by an ordinary pen filled with pure water as the ink (Fig. 7A–C). The handwritings are clearly visible under UV irradiation. If the handwritings are performed by alkaline ink (Na_2CO_3, 0.1 M), the induced fluorescence was even stronger. Text and patterns are highly distinct from the background as seen in Fig. 7D and E.

3.6. Thermoanalysis

Thermostability is highly desired for such materials in view of the high working temperature of paper and ink. TGA and DSC analysis were carried out to evaluate the thermostability of HABA. The TGA thermogram shows that HABA loses 5% of its weight at 261.45 °C (Fig. 8A and acquires the maximum decomposition rate at 280.17 °C, suggesting nice thermostability intrinsic to aromatic compounds. DSC analysis also substantiates the above claim. The DSC curve of HABA sample recorded is basically a straight line without any thermal effect (Fig. 8B), ruling out the possibility of phase transformation and thermal decomposition in the given scanning range (40–200 °C).

4. Conclusion

In summary, we have developed a luminogen (HABA) with specific solvent effect: turn-on stimuli-responsive fluorescence toward protic solvents. Owing to the presence of D-A pairs, polar solvents will bring the luminogen from the LE state to the CT state. While protic solvents will severely suppress the CT transition and simultaneously boost the LE transition. The reduction of CT in protic solvents rises from hydrogen bonding complexes as confirmed by DFT calculations as well as dynamic analysis. The stimuli-responsive can also be performed at solid state, in which the turn-on effect toward water- and base-ink is clearly visible under UV irradiation, enabling a new printing technique that has the advantages of green and convenience.

Acknowledgments

Support is acknowledged from the Beijing Municipal Education Commission Project (Grant No. KM201610028007 and KM201610028006) and National Natural Science Foundation of China (Grant No. 81573832).

Appendix A. Supplementary data

Supplementary data to this article can be found online at http://dx.doi.org/10.1016/j.saa.2017.04.079.

References

[1] T. Robert, Prog. Org. Coat. 78 (2015) 287.
[2] X.M. Du, T.Y. Li, L.J. Li, Z.C. Zhang, T.Z. Wu, J. Mater. Chem. C 3 (2015) 3542.
[3] L. Sheng, M.J. Li, S.Y. Zhu, H. Li, G. Xi, Y.G. Li, Y. Wang, Q.S. Li, S.J. Liang, K. Zhong, S.X.A. Zhang, Nat. Commun. 5 (2014)http://dx.doi.org/10.1038/Ncomms4044.
[4] W.S. Wang, N. Xie, L. He, Y.D. Yin, Nat. Commun. 5 (2014)http://dx.doi.org/10.1038/Ncomms6459.
[5] S. Magdassi, A. Bassa, Y. Vinetsky, A. Kamyshny, Chem. Mater. 15 (2003) 2208.
[6] K.G. Nair, D. Jayaseelan, P. Biji, RSC Adv. 5 (2015) 76092.
[7] Z. Stempien, E. Rybicki, T. Rybicki, J. Lesnikowski, Sensors Actuators B Chem. 224 (2016) 714.
[8] M. Blosi, S. Albonetti, F. Gatti, G. Baldi, M. Dondi, Dyes Pigments 94 (2012) 355.
[9] H.J. Sun, N. Gao, J.S. Ren, X.G. Qu, Chem. Mater. 27 (2015) 7573.
[10] D.R. Whang, Y. You, W.S. Chae, J. Heo, S. Kim, S.Y. Park, Langmuir 28 (2012) 15433.
[11] X.L. Zhu, R. Liu, Y.H. Li, H. Huang, Q. Wang, D.F. Wang, X. Zhu, S.S. Liu, H.J. Zhu, Chem. Commun. 50 (2014) 1359.
[12] T.Y. Han, X. Feng, D.D. Chen, Y.P. Dong, J. Mater. Chem. C 3 (2015) 7446.
[13] Z.G. Chi, X.Q. Zhang, B.J. Xu, X. Zhou, C.P. Ma, Y. Zhang, S.W. Liu, J.R. Xu, Chem. Soc. Rev. 41 (2012) 3878.
[14] Y.Q. Dong, J.W.Y. Lam, B.Z. Tang, J. Phys. Chem. Lett. 6 (2015) 3429.
[15] H.B. Sun, S.J. Liu, W.P. Lin, K.Y. Zhang, W. Lv, X. Huang, F.W. Huo, H.R. Yang, G. Jenkins, Q. Zhao, W. Huang, Nat. Commun. 5 (2014)http://dx.doi.org/10.1038/Ncomms4601.
[16] M. Irie, T. Fukaminato, T. Sasaki, N. Tamai, T. Kawai, Nature 420 (2002) 759.
[17] H.P. Diao, W.P. Niu, W. Liu, L.H. Feng, J. Xie, Spectrochim. Acta A 172 (2017) 65.
[18] J.B. Zhang, J.L. Chen, B. Xu, L.J. Wang, S.Q. Ma, Y.J. Dong, B. Li, L. Ye, W.J. Tian, Chem. Commun. 49 (2013) 3878.
[19] L.Y. Hu, Y.A. Duan, Z.Z. Xu, J. Yuan, Y.P. Dong, T.Y. Han, J. Mater. Chem. C 4 (2016) 5334.
[20] J.Y. Sun, J.Q. Han, Y. Liu, Y.A. Duan, T.Y. Han, J. Yuan, J. Mater. Chem. C 4 (2016) 8276.
[21] Y.J. Dong, B. Xu, J.B. Zhang, X. Tan, L.J. Wang, J.L. Chen, H.G. Lv, S.P. Wen, B. Li, L. Ye, B. Zou, W.J. Tian, Angew. Chem. Int. Ed. 51 (2012) 10782.
[22] T.Y. Han, Y.N. Hong, N. Xie, S.J. Chen, N. Zhao, E.G. Zhao, J.W.Y. Lam, H.H.Y. Sung, Y.P. Dong, B. Tong, B.Z. Tang, J. Mater. Chem. C 1 (2013) 7314.
[23] Q.F. Niu, X.X. Wu, T.D. Li, Y.Z. Cui, S.S. Zhang, X.Y. Li, Spectrochim. Acta A 163 (2016) 45.
[24] T. Pradhan, S. Maiti, R. Kumar, Y.H. Lee, J.W. Kim, J.H. Lee, J.S. Kim, Dyes Pigments 121 (2015) 1.
[25] E. Krystkowiak, K. Dobek, A. Maciejewski, Photochem. Photobiol. Sci. 12 (2013) 446.
[26] S. Chevreux, C. Allain, L. Wilbraham, K. Nakatani, P. Jacques, I. Ciofini, G. Lemercier, Faraday Discuss. 185 (2015) 285.
[27] D. Babusca, C. Morosanu, D.O. Dorohoi, Spectrochim. Acta A 172 (2017) 58.
[28] G.J. Zhao, K.L. Han, Acc. Chem. Res. 45 (2012) 404.
[29] R.R. Wei, P.S. Song, A.J. Tong, J. Phys. Chem. C 117 (2013) 3467.
[30] H.L. Liu, X.Y. Wang, Y. Xiang, A.J. Tong, Anal. Methods 7 (2015) 5028.
[31] C. Zhong, Phys. Chem. Chem. Phys. 17 (2015) 9248.
[32] S. Uchiyama, K. Takehira, T. Yoshihara, S. Tobita, T. Ohwada, Org. Lett. 8 (2006) 5869.
[33] A. Kobayashi, K. Takehira, T. Yoshihara, S. Uchiyama, S. Tobita, Photochem. Photobiol. Sci. 11 (2012) 1368.
[34] Y. Zhao, D.G. Truhlar, J. Phys. Chem. A 108 (2004) 6908.
[35] A. Chuma, H.W. Horn, W.C. Swope, R.C. Pratt, L. Zhang, B.G.G. Lohmeijer, C.G. Wade, R.M. Waymouth, J.L. Hedrick, J.E. Rice, J. Am. Chem. Soc. 130 (2008) 6749.